

MRI of Gallstones with Different Compositions

Hong-Ming Tsai¹
 Xi-Zhang Lin²
 Chiung-Yu Chen²
 Pin-Wen Lin³
 Jui-Che Lin⁴

OBJECTIVE. Gallstones are usually recognized on MRI as filling defects of hypointensity. However, they sometimes may appear as hyperintensities on T1-weighted imaging. This study investigated how gallstones appear on MRI and how their appearance influences the detection of gallstones.

MATERIALS AND METHODS. Gallstones from 24 patients who had MRI performed before the removal of the gallstones were collected for study. The gallstones were classified either as cholesterol gallstone ($n = 4$) or as pigment gallstone ($n = 20$) according to their gross appearance and based on analysis by Fourier transform infrared spectroscopy. MRI included three sequences: single-shot fast spin-echo T2-weighted imaging, 3D fast spoiled gradient-echo T1-weighted imaging, and in-phase fast spoiled gradient-echo T1-weighted imaging. The signal intensity and the detection rate of gallstones on MRI were further correlated with the character of the gallstones.

RESULTS. On T1-weighted 3D fast spoiled gradient-echo images, most of the pigment gallstones (18/20) were hyperintense and all the cholesterol gallstones (4/4) were hypointense. The mean ratio of the signal intensity of gallstone to bile was (\pm standard deviation) 3.36 ± 1.88 for pigment gallstone and 0.24 ± 0.10 for cholesterol gallstone on the 3D fast spoiled gradient-echo sequence ($p < 0.001$). Combining the 3D fast spoiled gradient-echo and single-shot fast spin-echo sequences achieved the highest gallstone detection rate (96.4%).

CONCLUSION. Based on the differences of signal intensity of gallstones, the 3D fast spoiled gradient-echo T1-weighted imaging was able to diagnose the composition of gallstones. Adding the 3D fast spoiled gradient-echo imaging to the single-shot fast spin-echo T2-weighted sequence can further improve the detection rate of gallstones.

Gallstones are usually depicted on MRI by the characteristic signal void from the stones contrasted against the high signal from the surrounding bile. This phenomenon may be observed on T2-weighted spin-echo images or T1-weighted images of a patient who has been fasting and has high signal from concentrated bile [1, 2]. Nonetheless, gallstones may show high-signal-intensity areas in their centers on T2-weighted MRI, and this intensity is thought to be caused by water-filled clefts in such gallstones [3, 4]. However, other factors contributing to the hyperintensity of gallstones on MRI are still possible [5–10]. Moeser et al. [6] first reported a case of hyperintense gallstones on T1-weighted imaging, which was confirmed later by similar findings of other investigators [5, 7–9]. Based on the result of an in vitro study, Ukaji et al.

[10] concluded that metal ions in pigment gallstones caused the hyperintensity of gallstones on T1-weighted MRI. However, no study to date has ever correlated the in vivo MRI appearance of gallstones with their composition and assessed the impact of their MRI appearance on detection. This study was, therefore, aimed to investigate MRI of patients with either cholesterol or pigment gallstones and to assess the influence of variability of MRI on gallstone detection.

Materials and Methods

Gallstones

From August 2001 to March 2003, patients who had gallstones removed by surgery and who also had MRI performed before surgery were enrolled in this study. In total, 24 patients were enrolled (15 men and nine women) with a mean age of 63.8

Received August 18, 2003; accepted after revision December 7, 2003.

¹Department of Radiology, National Cheng Kung University Hospital, Tainan 704, Taiwan.

²Department of Internal Medicine, National Cheng Kung University Hospital, 138 Sheng-Li Rd., Tainan 704, Taiwan. Address correspondence to C.-Y. Chen (chiungyu@mail.ncku.edu.tw).

³Department of Surgery, National Cheng Kung University Hospital, Tainan 704, Taiwan.

⁴Department of Chemical Engineering, College of Engineering, National Cheng Kung University, Tainan 704, Taiwan.

AJR 2004;182:1513–1519

0361–803X/04/1826–1513

© American Roentgen Ray Society

years (range, 32–83 years). Stones were found solely in the gallbladder in 12 patients, in the intrahepatic ducts in four patients, and in the common bile duct in two patients. Aside from these stones, six patients had common bile duct stones combined with either gallbladder stones ($n = 5$) or intrahepatic duct stones ($n = 1$). The size of gallstones ranged from 2 to 35 mm with a mean diameter (\pm standard deviation [SD]) of 10.6 ± 7.7 mm.

The gallstones were washed with normal saline and maintained in airtight plastic bottles to avoid transformation of the gallstone structure by drying. The gallstones were classified as cholesterol stones or pigment stones according to their surface and cutting plane as described by the gallstone classification of the Japanese Study Group (1986) [11]. The gallstones were further examined by Fourier transform infrared spectroscopy on a Fourier transform infrared (FTIR) spectrometer (FTS-40, Bio-Rad) for wave number 4,000 to 400 cm^{-1} and a spectral resolution of 8 cm^{-1} . Potassium bromide pellets were used to generate the background spectra. The chemical compositions were then compared to the spectra of calcium bilirubinate, calcium carbonate, and calcium palmitate.

In Vivo Imaging

MRI was performed using a field strength of 1.5 T on an MRI system (Signa CV/i, General Electric Medical Systems) with a phased array torso coil. Two fast spoiled gradient-echo T1-weighted images and a single-shot fast spin-echo T2-weighted image were obtained. For in-phase fast spoiled gradient-echo images, the parameters were TR range/TE, 175–185/4.2; slice thickness, 8 mm; gap, 2 mm; and flip angle, 90°. For 3D fast spoiled gradient-echo images, the parameters were TR/TE, 5.9/1.2; slice thickness, 6 mm; 3-mm overlap between each image; and flip angle, 10°. For single-shot fast spin-echo T2 images, the parameters were TR range/TE range, 20,000–25,000/90–100; slice thickness, 8

mm; and gap, 2 mm. The 3D fast spoiled gradient-echo images were acquired with fat saturation, and the in-phase fast spoiled gradient-echo images were not. All the sequences used a field of view as adjusted by the patients' respective body sizes and a 256×168 matrix. The gallstone images obtained using the different sequences were analyzed for the presence and signal intensity of gallstones.

In Vitro Imaging

The gallstones were placed in a normal saline suspension in individual plastic bottles and embedded in water-immersed custom floral foam as a body phantom for MRI. In vitro MRI used the same sequences and parameters as the set for the in vivo MRI except that the slice thickness was 5 mm and an additional set of in-phase fast spoiled gradient-echo images with fat saturation was also obtained.

The gallstones were first pulverized and desiccated before the MRI was performed to analyze the contribution of water content in the signal intensity of gallstones on MRI. The homogeneous gallstone powder was placed individually in the plastic Eppendorf tube and embedded in water-immersed custom floral foam as a body phantom for MRI. The setting used for the MRI was the same as that described for the in vitro study. MRI was repeated after adding normal saline to the desiccated gallstone powder to confirm the influence of water on the signal intensity rather than that of any structural change during the process of desiccation. The appearance and signal intensity of the gallstones were recorded for further analysis.

Measurement of Signal Intensity

Quantitative assessment of the signal intensity on T1- and T2-weighted sequences was obtained through operator-defined regions of interest. The gallstone signal intensity was measured and compared with the intensity of the gallbladder bile, re-

sulting in a stone–bile signal intensity ratio for each gallstone. Signal intensity was measured at the bile of the dilated common bile duct in three patients who underwent cholecystectomy earlier. If the intensity of a gallstone's magnetic resonance signal varied throughout its structure, it was measured at its most intense region.

In vitro measurement of signal intensity was similar to the in vivo study except that the signal intensity was measured either at the gallstones and surrounding saline or at the gallstone powder and the water-immersed floral foam phantom.

Statistical Analysis

The value of signal intensity ratio was expressed as mean \pm 1 SD. The differences in the signal intensity ratio between the cholesterol and pigment gallstone groups were examined by the Mann-Whitney U test. The detection rates of gallstones on different MRI sequences were compared using the chi-square test. A p value of less than 0.05 was considered to be statistically significant. The statistical calculations were computed using SPSS version 8.0 (Statistical Package for the Social Sciences) for Windows (Microsoft).

Results

All the black and brown stones (classified by the gallstone classification of the Japanese Study Group [11]) showed broad peaks on FTIR analysis corresponding to calcium bilirubinate in the absorbency region 1,600–1,640 cm^{-1} and calcium palmitate in the absorbency region 2,900–2,940 cm^{-1} . No discrepancy was found between the results of gallstone classification as determined by the gallstone's gross appearance and by FTIR analysis. In total, 20 patients had pigment gallstones and four patients had cholesterol gallstones.

As shown in Table 1, 90% and 30% of the pigment gallstones were hyperintense on the in vivo T1-weighted 3D fast spoiled gradient-echo (Fig. 1A) and in-phase fast spoiled gradient-echo images, respectively, and all the cholesterol gallstones were hypointense on the T1-weighted images (Figs. 2A and 2B). All the gallstones appeared as hypointensities on the T2-weighted single-shot fast spin-echo images (Figs. 1C and 2C). The in vivo (Figs. 1A–1C and Figs. 2A–2C) and in vitro (Figs. 1D–1G and Figs. 2D–2G) images of gallstones were similar but differed in that more pigment gallstones were hyperintense on the in vitro T1-weighted in-phase fast spoiled gradient-echo images.

As listed in Table 2, the contrast of signal intensity between the pigment gallstones and the background was prominent on either the

TABLE 1 In Vivo and In Vitro MRI Appearances of Gallstones

Imaging Technique	Cholesterol Gallstone			Pigment Gallstone		
	Increased Signal	Isointense	Decreased Signal	Increased Signal	Isointense	Decreased Signal
3D Fast spoiled gradient-echo						
In vivo	0	0	4	18	1	1
In vitro	0	0	4	19	0	1
In-phase fast spoiled gradient-echo						
In vivo	0	0	4	6	13	1
In vitro	0	0	4	18	0	2
Single-shot fast spin-echo						
In vivo	0	0	4	0	2	18
In vitro	0	0	4	0	0	20

MRI of Gallstones

in vivo or the in vitro 3D fast spoiled gradient-echo images and became less prominent on the T1-weighted in-phase fast spoiled gradient-echo images with and without fat saturation. The signal intensity of cholesterol gallstones was lower than that of the background on both T1- and T2-weighted MR images. The mean ratios of stone-to-background signal intensities of pigment and cholesterol gallstones were therefore significantly different on the 3D fast spoiled gradient-echo and in-phase fast spoiled gradient-echo T1-weighted images but were similar on the T2-weighted single-shot fast spin-echo images.

Table 3 shows the effect of the water content on gallstone MRI. The desiccated powders of all cholesterol and pigment stones were hypointense on T1-weighted imaging.

The intensities of the pigment gallstone powders on T1-weighted images were so greatly enhanced after adding normal saline that the mean intensity of pigment gallstones was 4.36 and 3.86 times greater, respectively, to that of body phantom on 3D fast spoiled gradient-echo and in-phase fast spoiled gradient-echo sequences. However, the mean intensity of cholesterol gallstone was only slightly enhanced after the addition of normal saline with a mean signal intensity ratio of stone-to-body phantom of approximately 1 on T1-weighted images. Both the pigment and cholesterol gallstone powders were hypointense on T2-weighted images, and the signal intensities were lower than that of the body phantom, whether before or after the addition of normal saline.

Table 4 shows the results of MRI diagnosis of gallstone using different MRI sequences. The cholesterol gallstones exclusively occurred in the gallbladder in our collections and were visualized as filling defects on all three MRI sequences (Figs. 2A–2C). The T2-weighted single-shot fast spin-echo imaging showed pigment gallstone as a filling defect and was good in detecting those gallbladder stones. The T1-weighted 3D fast spoiled gradient-echo imaging presented the pigment gallstones as hyperintense areas and was good in detecting those common bile duct stones (Fig. 1A). The T1-weighted 3D fast spoiled gradient-echo MRI missed a gallbladder stone and the T2-weighted single-shot fast spin-echo MRI missed two common bile duct stones. Moreover, both the T1- and T2-

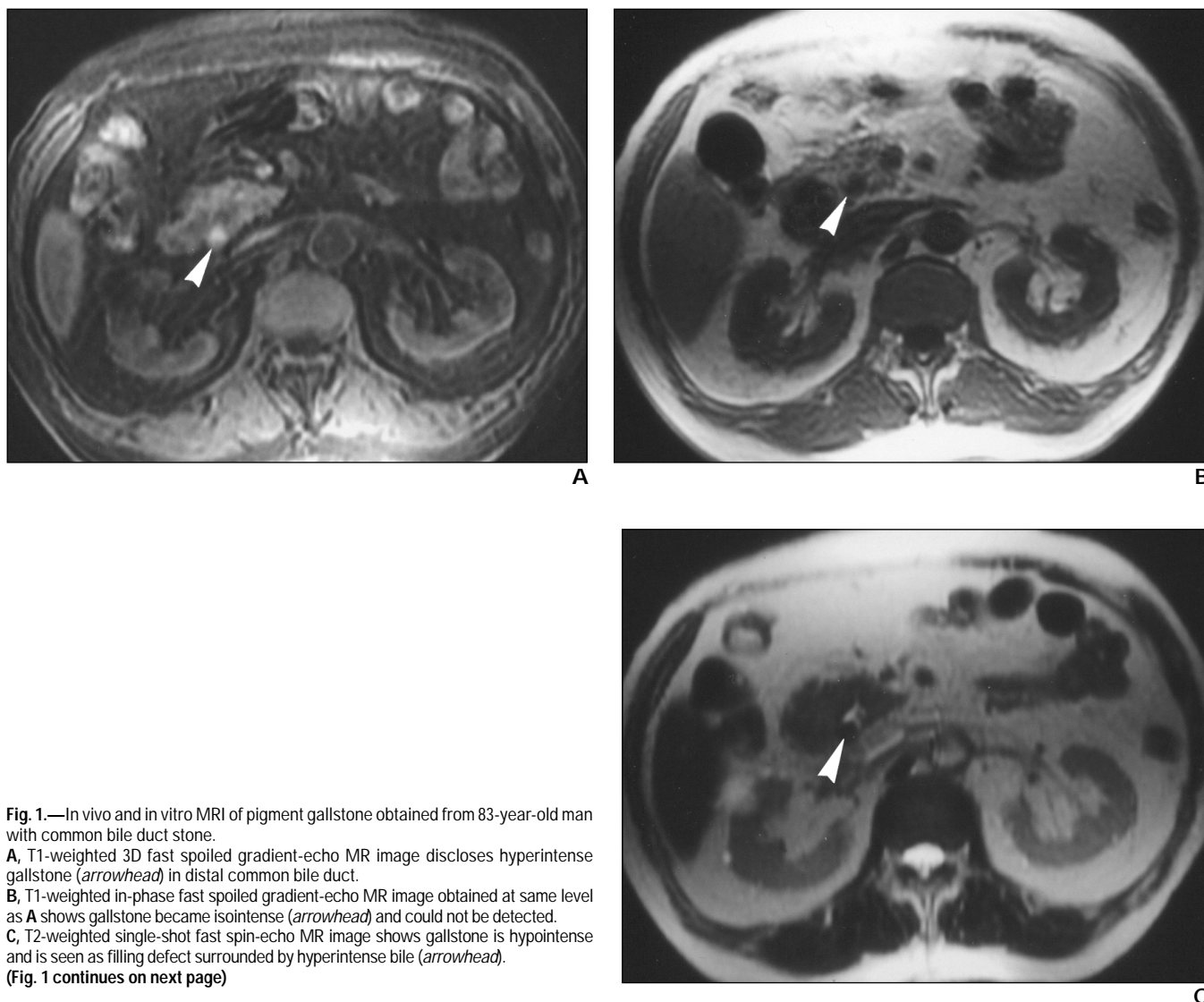


Fig. 1.—In vivo and in vitro MRI of pigment gallstone obtained from 83-year-old man with common bile duct stone.

A, T1-weighted 3D fast spoiled gradient-echo MR image discloses hyperintense gallstone (*arrowhead*) in distal common bile duct.

B, T1-weighted in-phase fast spoiled gradient-echo MR image obtained at same level as **A** shows gallstone became isointense (*arrowhead*) and could not be detected.

C, T2-weighted single-shot fast spin-echo MR image shows gallstone is hypointense and is seen as filling defect surrounded by hyperintense bile (*arrowhead*).

(**Fig. 1** continues on next page)

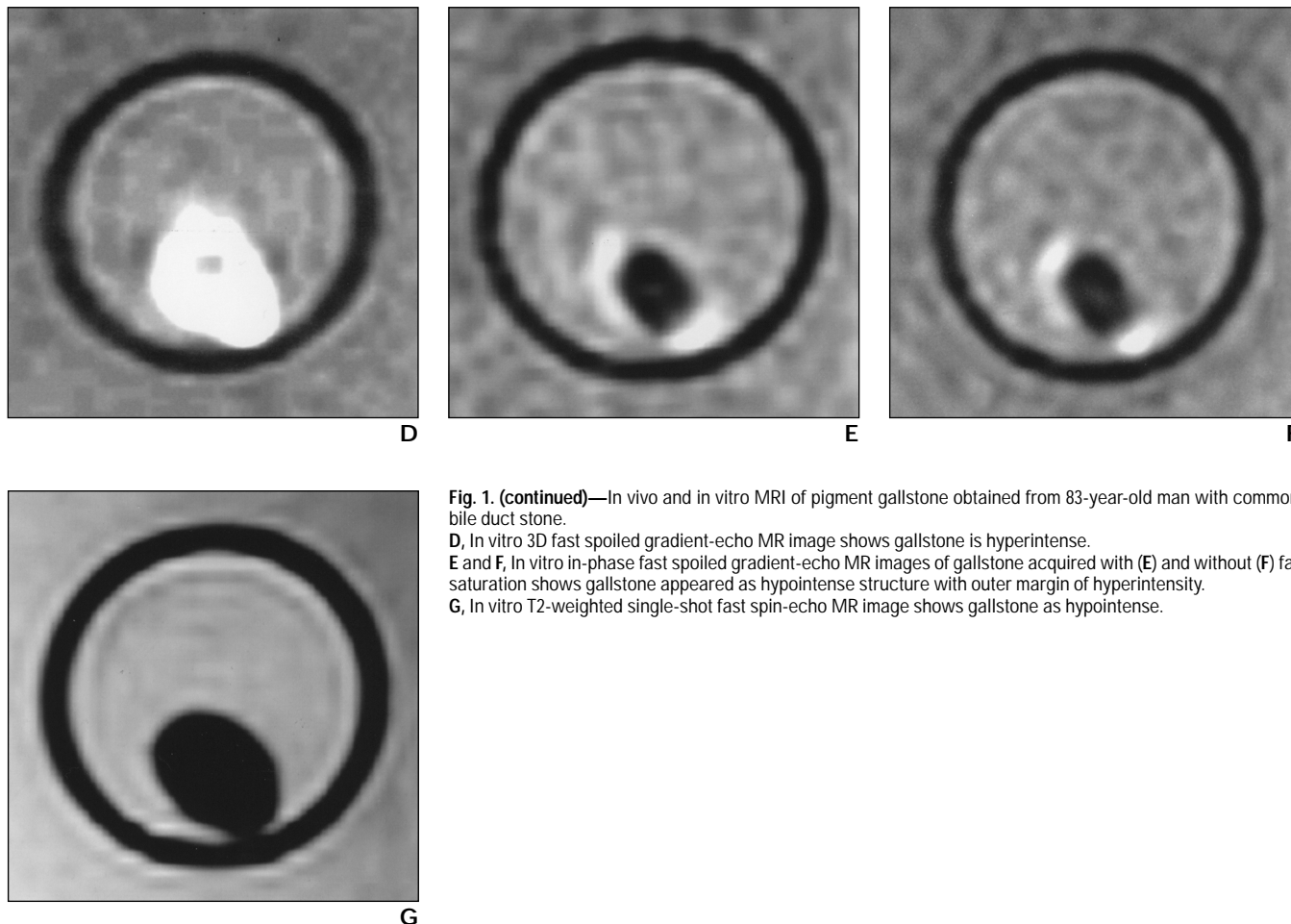


Fig. 1. (continued)—In vivo and in vitro MRI of pigment gallstone obtained from 83-year-old man with common bile duct stone.

D, In vitro 3D fast spoiled gradient-echo MR image shows gallstone is hyperintense.

E and F, In vitro in-phase fast spoiled gradient-echo MR images of gallstone acquired with (E) and without (F) fat saturation shows gallstone appeared as hypointense structure with outer margin of hyperintensity.

G, In vitro T2-weighted single-shot fast spin-echo MR image shows gallstone as hypointense.

weighted MRI missed detecting a case of intrahepatic duct stones, which were isointense pigment stones 5 mm in diameter and appearing in a nondilated bile duct. Because more than half the pigment gallstones appeared isointense on T1-weighted in-phase fast spoiled gradient-echo images (Table 1), the in-phase fast spoiled gradient-echo imaging was not good for the detection of pigment gallstone. Combining the 3D fast spoiled gradient-echo and the single-shot fast spin-echo MRI sequences achieved the highest rate of gallstone detection.

Discussion

MR cholangiography detects bile duct stones as areas of signal void in the high-signal-intensity bile and has been the diagnostic tool of choice for detecting gallstones. However, symptoms relating to bile duct stones may be nonspecific and can be merely bile duct dilatation without fever and abdominal pain [12]. Abdominal MRI may therefore be

performed for gallstone patients with atypical symptoms. Because MRI usually includes axial T1- and T2-weighted sequences, the recognition of bile duct stones on these sequences as the cause of symptoms, or as coincidental findings, would be beneficial.

T2-weighted imaging has been considered superior to T1-weighted imaging in detecting bile duct stones because most of the gallstones are isointense on T1-weighted MR images [13]. Although only some gallstones have been reported to be hyperintense on T1-weighted imaging [5–10], a considerable number of stones have appeared as hyperintensities on our T1-weighted imaging. Gallstones of hyperintensity on T1-weighted images have been found to be related to stones having brown to black cross sections or a salt-and-pepper appearance [6, 10]. These stones, according to the gallstone classification of the Japanese Study Group [11], should be classified as pigment gallstones. As seen in our study, the intensity ratio of gallstone to bile or to normal saline of the

T1-weighted imaging was significantly higher for pigment gallstones than for cholesterol gallstones. These findings show that the hyperintense gallstones on T1-weighted images were pigment gallstones and cholesterol gallstones were exclusively hypointense on T1-weighted imaging.

Differentiation of pigment and cholesterol gallstones was once important 10–20 years ago, when gallstone dissolution therapy was popular for patients with gallbladder stones. At that time, diagnosis of the composition of the gallstone was important in predicting the success of gallstone dissolution and in choosing the solvent for gallstone dissolution. The advent of laparoscopic cholecystectomy, however, has changed that. Currently, few patients with gallstones are treated with dissolution therapy. Nevertheless, because of the different consistencies of cholesterol and pigment gallstones, the differentiation of gallstone composition may still have a clinical impact when dealing with endoscopic mechanical lithotripsy for big common bile

MRI of Gallstones

duct stones. On such an occasion, the big pigment gallstone can be easily crushed by a mechanical lithotripter and retrieved, whereas the presence of big cholesterol gallstones usually implies a difficult-to-treat stone because they are harder than pigment stones and endoscopic lithotripsy may fail.

Ukaji et al. [10] studied the in vitro images of gallstones and considered that the hyperintensity of pigment gallstone on T1-weighted images was caused by the presence of metal ions in the pigment stones. These metal ions behave as paramagnetic ions, shortening the T1 relaxation time of water protons, and as such, stones containing these ions appeared as hyperintense areas on T1-weighted images. The presence of water, therefore, plays a key role in determining the intensity of gallstones on MRI. This theory was further tested and supported by our study, showing that all pigment gallstones

became signal void on T1-weighted imaging after desiccation, whereas the hyperintensity of pigment gallstones was restored after adding normal saline.

We found that most of the pigment gallstones were hyperintense on the T1-weighted 3D fast spoiled gradient-echo images, although only one third of them were hyperintense on the T1-weighted in-phase fast spoiled gradient-echo images. Because the 3D fast spoiled gradient-echo images were acquired with fat saturation and the in-phase fast spoiled gradient-echo images were not, the higher intensity of gallstone on 3D fast spoiled gradient-echo images may be caused by fat saturation itself, which increased the apparent brightness of water-bearing stones. Such inference, however, has been discounted because the in vitro in-phase fast spoiled gradient-echo images showed similar image and intensity ratio acquired either

with or without fat saturation. The 3D fast spoiled gradient-echo MRI sequence differs from the in-phase fast spoiled gradient-echo sequence not only in the thickness of the slice but also in the TE and TR. As seen in the previous ferumoxides experiment, the short TE of 3D fast spoiled gradient-echo sequence may reduce the susceptibility and short transverse relaxation effect of the metal ions and therefore increase the signal of pigment gallstones [14]. The TR of the 3D fast spoiled gradient-echo sequence being shorter than the in-phase fast spoiled gradient-echo sequence may contribute to a suppression of the background signal and result in improved visualization of the longitudinal effect of gallstones containing metal ions [14]. Because the 3D fast spoiled gradient-echo sequence is not used for routine MRI diagnosis of gallstone, its application in our study should account for the higher incidence of

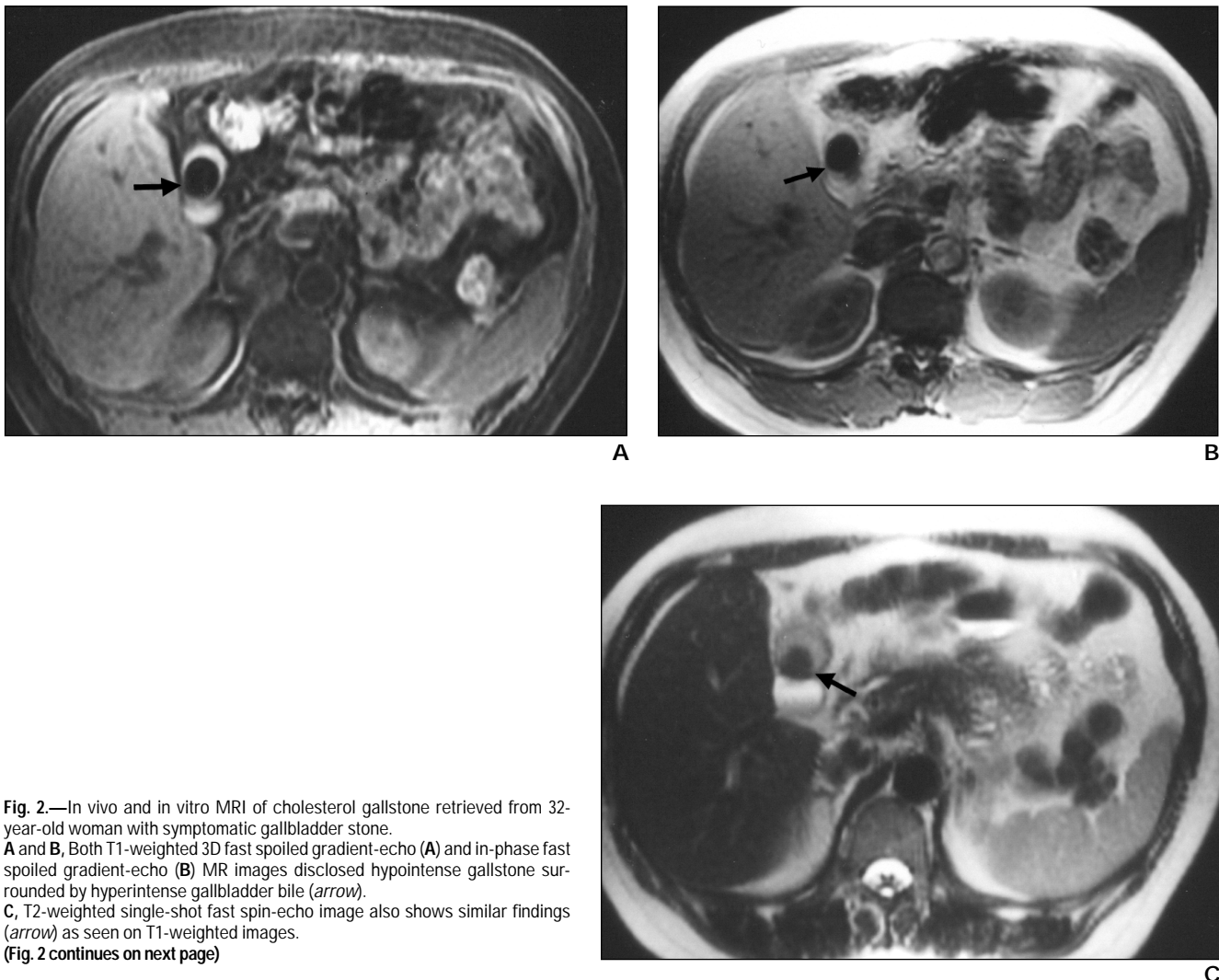


Fig. 2.—In vivo and in vitro MRI of cholesterol gallstone retrieved from 32-year-old woman with symptomatic gallbladder stone. **A and B,** Both T1-weighted 3D fast spoiled gradient-echo (**A**) and in-phase fast spoiled gradient-echo (**B**) MR images disclosed hypointense gallstone surrounded by hyperintense gallbladder bile (*arrow*). **C,** T2-weighted single-shot fast spin-echo image also shows similar findings (*arrow*) as seen on T1-weighted images. (**Fig. 2 continues on next page**)

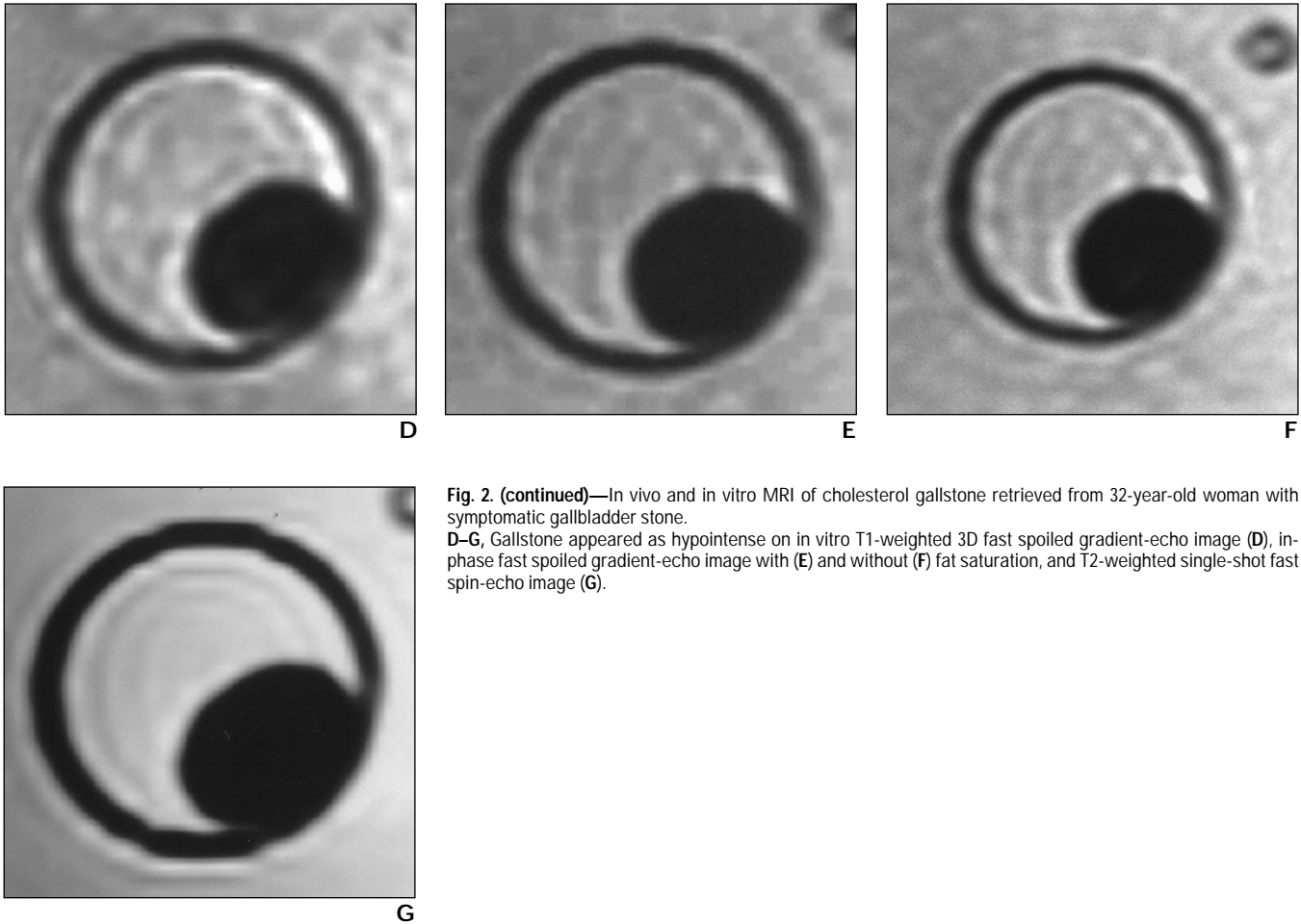


Fig. 2. (continued)—In vivo and in vitro MRI of cholesterol gallstone retrieved from 32-year-old woman with symptomatic gallbladder stone. **D–G**, Gallstone appeared as hypointense on in vitro T1-weighted 3D fast spoiled gradient-echo image (**D**), in-phase fast spoiled gradient-echo image with (**E**) and without (**F**) fat saturation, and T2-weighted single-shot fast spin-echo image (**G**).

hyperintense gallstones in our study than in other reports.

MR cholangiography and T2-weighted MRI detect gallstones indirectly by showing them as filling defects. However, several pit-

falls are associated with them. First, other types of intraluminal filling defects, such as intraductal tumor, blood clot, or gas bubble (pneumobilia), can mimic gallstones and may be difficult to differentiate [15]. Second, gall-

stones impacted at the ampulla may be missed on T2-weighted imaging because of the lack of bile surrounding the stone and, hence, no filling defect will appear on the images [15]. These pitfalls can be avoided by using T1-weighted 3D fast spoiled gradient-echo imaging because it reveals pigment gallstones directly as hyperintense areas on images rather than just as filling defects. This characteristic of T1-weighted 3D fast spoiled gradient-echo imaging explains why the 3D fast spoiled gradient-echo sequence is better than the single-shot fast spin-echo sequence for MRI in terms of diagnosing common bile duct stones in our study.

In summary, our study shows the MRI characteristics of cholesterol and pigment gallstones. In addition to recognizing a gallstone as a filling defect on T2-weighted single-shot fast spin-echo imaging, the cholesterol and pigment gallstones can be readily differentiated because most pigmented stones are bright, whereas cholesterol stones are dark on 3D fast spoiled gradient-echo T1-

TABLE 2 Signal Contrast of Gallstones to Gallbladder Bile and Normal Saline for In Vivo and In Vitro MRI				
Imaging Technique	In Vivo		In Vitro	
	Cholesterol Gallstone	Pigment Gallstone	Cholesterol Gallstone	Pigment Gallstone
3D Fast spoiled gradient-echo	0.24 ± 0.10	3.36 ± 1.88 ^a	0.30 ± 0.16	3.38 ± 1.72 ^a
In-phase fast spoiled gradient-echo	0.27 ± 0.13	1.38 ± 0.90 ^b	0.31 ± 0.19	1.86 ± 0.81 ^b
In-phase fast spoiled gradient-echo with fat saturation	—	—	0.24 ± 0.10	1.97 ± 0.66 ^a
Single-shot fast spin-echo	0.26 ± 0.07	0.40 ± 0.27	0.23 ± 0.13	0.30 ± 0.21

Note.—Data are expressed as mean ± standard deviation. Dash (—) indicates no data available.

^a*p* = 0.001.

^b*p* = 0.02, Mann-Whitney *U* test.

MRI of Gallstones

TABLE 3 Signal Contrast of Gallstone Powder to Body Phantom With and Without Normal Saline

Imaging Technique	Without Normal Saline		With Normal Saline	
	Cholesterol Gallstone	Pigment Gallstone	Cholesterol Gallstone	Pigment Gallstone
3D Fast spoiled gradient-echo	0.058 ± 0.022	0.082 ± 0.038	1.25 ± 0.12	4.36 ± 1.06 ^a
In-phase fast spoiled gradient-echo	0.17 ± 0.06	0.17 ± 0.05	1.00 ± 0.20	3.86 ± 1.28 ^a
Single-shot fast spin-echo	0.064 ± 0.033	0.042 ± 0.021	0.46 ± 0.27	0.19 ± 0.21 ^b

Note.—Data expressed as mean ± standard deviation.

^a*p* = 0.001.

^b*p* = 0.02, Mann-Whitney *U* test.

TABLE 4 Detection Rate of Gallstones in Different Locations of the Biliary Tree on MRI

Imaging Technique	Cholesterol Gallstone in Gallbladder (<i>n</i> = 4)	Pigment Gallstone			Total (<i>n</i> = 28)
		Gallbladder (<i>n</i> = 11)	Common Bile Duct (<i>n</i> = 8)	Intrahepatic Bile Duct (<i>n</i> = 5)	
3D Fast spoiled gradient-echo	4 (100)	10 (90.9)	8 (100)	4 (80)	26 (92.9) ^a
In-phase fast spoiled gradient-echo	4 (100)	2 (18.2)	2 (25)	3 (60)	11 (39.3)
Single-shot fast spin-echo	4 (100)	11 (100)	6 (75)	4 (80)	25 (89.3) ^a
Combined single-shot fast spin-echo and 3D fast spoiled gradient-echo ^a	4 (100)	11 (100)	8 (100)	4 (80)	27 (96.4)

Note.—Data are expressed as number of patients with detection rate in parentheses (%).

^a*p* = 0.003 by chi-square test between in-phase fast spoiled gradient-echo and other two sequences.

weighted imaging. The 3D fast spoiled gradient-echo T1-weighted imaging is as good as T2-weighted single-shot fast spin-echo imaging in diagnosing gallstones and can even be better when applied to bile duct stones. Common bile duct and intrahepatic duct stones are frequently pigment gallstones and are prevalent in many areas of Asia. We recommend a

combined use of 3D fast spoiled gradient-echo and single-shot fast spin-echo sequence for routine MRI of gallstones.

References

- Hricak H, Filly RA, Margulis AR, Moon KL, Crooks LE, Kaufman L. Work in progress: nuclear magnetic resonance imaging of the gallblad-

der. *Radiology* 1983;147:481-484

- McCarthy S, Hricak H, Cohen M, et al. Cholecystitis: detection with MR imaging. *Radiology* 1986;158:333-336
- Moon KL Jr, Hricak H, Margulis AR, et al. Nuclear magnetic resonance imaging characteristics of gallstones in vitro. *Radiology* 1983;148:753-756
- Moriyasu F, Ban N, Nishida O, et al. Central signals of gallstones in magnetic resonance imaging. *Am J Gastroenterol* 1987;82:139-142
- Baron RL, Shuman WP, Lee SP, et al. MR appearance of gallstones in vitro at 1.5 T: correlation with chemical composition. *AJR* 1989;153:497-502
- Moeser PM, Julian S, Karstaedt N, Strech M. Unusual presentation of cholelithiasis on T1-weighted MR imaging. *J Comput Assist Tomogr* 1988;12:150-152
- Mathieu D, Guinet C, Cauquil P, Vasile N, Roche A. Intrahepatic calculi: imaging by MR. *Radiat Med* 1988;6:1-8
- Zangger P, Grossholz M, Mentha G, Lemoine R, Graf JD, Terrier F. MRI findings in Caroli's disease and intrahepatic pigmented calculi. *Abdom Imaging* 1995;20:361-364
- Gabata T, Kadoya M, Matsui O, Kobayashi T, Sanada J, Mori A. Intrahepatic biliary calculi: correlation of unusual MR findings with pathologic findings. *Abdom Imaging* 2000;25:266-268
- Ukaji M, Ebara M, Tsuchiya Y, et al. Diagnosis of gallstone composition in magnetic resonance imaging in vitro analysis. *Eur J Radiol* 2002; 41:49-56
- Kitayama O, Ise H, Abe H, et al. Diagnosis of the types of gallstones by DIC [in Japanese]. *J Biliary Tract Pancreas* 1991;12:1191-1197
- Britton J, Bickerstaff KI, Savage A. Benign diseases of the biliary tract. In: Morris PJ, Malt RA, eds. *Oxford textbook of surgery*. Oxford, England: Oxford University Press, 1994:1209-1239
- Chan YL, Lam WW, Metreweli C, Chung SC. Detectability and appearance of bile duct calculus on MR imaging of the abdomen using axial T1- and T2-weighted sequences. *Clin Radiol* 1997;52:351-355
- Takahama K, Amano Y, Hayashi H, Kumazaki T. T1-weighted magnetic resonance imaging sequence appropriate for the evaluation of the longitudinal relaxation effect of superparamagnetic iron oxide: a phantom study. *J Nippon Med Sch* 2002;69:571-576
- Baillie J, Paulson EK, Vitellas KM. Biliary imaging: a review. *Gastroenterology* 2003;124:1686-1699